THE JOURNAL OF BIOLOGICAL CHEMISTRY VOL. 287, NO. 3, pp. 1679–1687, January 13, 2012

Role of Junctin Protein Interactions in Cellular Dynamics of Calsequestrin Polymer upon Calcium Perturbation*[S]

Received for publication, April 22, 2011, and in revised form, November 24, 2011 Published, JBC Papers in Press, November 28, 2011, DOI 10.1074/jbc.M111.254045

Keun Woo Lee[‡1], Jin-Soo Maeng[§1], Jeong Yi Choi[‡], Yu Ran Lee[‡], Chae Young Hwang[‡], Sung Sup Park[‡], Hyun Kyu Park[¶], Bong Hyun Chung[¶], Seung-Goo Lee[‖], Yeon-Soo Kim[**], Hyesung Jeon[‡‡], Soo Hyun Eom[§§], ChulHee Kang[¶¶], Do Han Kim[§§], and Ki-Sun Kwon[‡2]

From the [‡]Laboratory of Cell Signaling, Aging Research Center, [¶]Bio-Nanotechnology Research Center, and [‖]Industrial Biotechnology and Bioenergy Research Center, Korea Research Institute of Bioscience and Biotechnology (KRIBB), Daejeon 305-806, Korea, the [§]Bio-Nanotechnology Research Center, Korea Food Research Institute (KFRI), Gyeonggi-Do 463-746, Korea, the [**]Department of Smart Foods and Drugs and Indang Institute of Molecular Biology, Inje University, Seoul 100-032, Korea, the [‡‡]Biomedical Research Center, Korea Institute of Science and Technology, Seoul 136-791, Korea, the [§§]School of Life Sciences, Gwangju Institute of Science and Technology, Gwangju 500-712, Korea, and the [¶¶]Department of Chemistry, Washington State University, Pullman, Washington 99163

Background: *In vitro* studies have reported reversible calsequestrin polymerization and depolymerization.
Results: Live cell imaging analysis revealed Ca^{2+}-dependent decondensation of calsequestrin speckles, consistent with *in vitro* microscopic data.
Conclusion: Calsequestrin depolymerization by calcium depletion requires coexistence of junctin.
Significance: The role of calsequestrin in intracellular calcium homeostasis was explored.

Calsequestrin (CSQ), the major intrasarcoplasmic reticulum calcium storage protein, undergoes dynamic polymerization and depolymerization in a Ca^{2+}-dependent manner. However, no direct evidence of CSQ depolymerization *in vivo* with physiological relevance has been obtained. In the present study, live cell imaging analysis facilitated characterization of the *in vivo* dynamics of the macromolecular CSQ structure. CSQ2 appeared as speckles in the presence of normal sarcoplasmic reticulum (SR) Ca^{2+} that were decondensed upon Ca^{2+} depletion. Moreover, CSQ2 decondensation occurred only in the stoichiometric presence of junctin (JNT). When expressed alone, CSQ2 speckles remained unchanged, even after Ca^{2+} depletion. FRET analysis revealed constant interactions between CSQ2 and JNT, regardless of the SR Ca^{2+} concentration, implying that JNT is an essential component of the CSQ scaffold. *In vitro* solubility assay, electron microscopy, and atomic force microscopy studies using purified recombinant proteins confirmed Ca^{2+} and JNT-dependent disassembly of the CSQ2 polymer. Accordingly, we conclude that reversible polymerization and depolymerization of CSQ are critical in SR Ca^{2+} homeostasis.

Sarcoplasmic reticulum (SR)[3] is a major Ca^{2+} storage reservoir in muscle. The SR Ca^{2+} release channel, ryanodine receptor (RyR), forms a large macromolecular complex with transmembrane, luminal, and cytoplasmic components (1). RyR recruits a low affinity (K_d = 1 mM), high capacity (60–80 mol Ca^{2+} mol^{-1}) Ca^{2+}-binding protein, calsequestrin (CSQ), to sense the environment within SR (2). CSQ1 is predominantly expressed in fast-twitch skeletal muscle, and CSQ2 is predominantly expressed in slow-twitch skeletal and cardiac muscle (3). Membrane-spanning proteins, triadin (TRN) and junctin (JNT) (4, 5), bind to both CSQ and RyR and presumably facilitate communication between CSQ and RyR channel (6). The N-terminal regions of these proteins are located in the cytoplasm and the C-terminal regions in the lumen of the SR. The luminal domain of these proteins containing the KEKE repeat is proposed to directly interact with CSQ (5). Thus, CSQ, TRN, and JNT play an active role in relaying information on the Ca^{2+} load in the SR to RyR so that resting and voltage-activated Ca^{2+} release can be modified in response to changes in the store load through physical coupling between these proteins (7). However, the individual steps constituting this system remain to be established.

Catecholamine-induced polymorphic ventricular tachycardia (CPVT) is a familial arrhythmogenic disorder caused by the aberrant release of Ca^{2+} from the SR. CPVT is linked to a defective channel, either RyR2 itself or other regulatory components of the channel gating machinery. Mutations in RyR2 and CSQ2 are linked to CPVT. In total, seven CSQ2 mutations have been identified in association with CPVT (8–11). Moreover, abnormal expression of JNT and TRN is associated with the CPVT pattern (12).

Human CSQ2, containing 391 amino acids plus a 19-residue N-terminal signal peptide, is highly acidic due to enrichment of

* This work was supported by grants from the Ministry of Education, Science and Technology (Grants 2011-0002141, 2011-0030134, and 2011-0027762) (to K. S. K.) and a grant from the Systems Biology Infrastructure Gwangju Institute of Science and Technology (to S. H. E., H. J., and D. H. K.).
[S] This article contains supplemental Movies S1 and S2 and Figs. S1 and S2.
[1] Both authors contributed equally to this work.
[2] To whom correspondence should be addressed: Laboratory of Cell Signaling, Aging Research Center, Korea Research Institute of Bioscience and Biotechnology, 125 Gwahangno, Yusong, Daejeon 305-806, Korea. Tel.: 82-42-860-4143; Fax: 82-42-879-8596; E-mail: kwonks@kribb.re.kr.
[3] The abbreviations used are: SR, sarcoplasmic reticulum; SERCA, sarco/endoplasmic reticulum Ca^{2+} ATPase; CSQ, calsequestrin; JNT, junctin; RyR, ryanodine receptor; TRN, triadin; CPVT, catecholamine-induced polymorphic ventricular tachycardia; AFM, atomic force microscopy.

acidic residues (60%) within the 63 carboxyl-terminal amino acids. Although human CSQ1 and CSQ2 are the products of different genes, the proteins display 65% sequence identity, are acidic, and share one glycosylation site. However, CSQ2 contains a 31-amino acid extension at its carboxyl terminus (residues 361–391) comprising 71% acidic residues, which significantly contributes to its ability to bind large amounts of Ca^{2+} (13), as well as a second glycosylation site. CSQ exists either as a monomer or as a wide range of polymers, depending on the Ca^{2+} concentration. The extended N terminus of CSQ establishes a front-to-front dimer interface through arm exchange. The C terminus of CSQ, the most negative region, is critical in forming tetrameric and higher-order linear polymers and capturing Ca^{2+} in the back-to-back interface (14–16). Wang *et al.* (17) demonstrated that knockdown of CSQ2, but not CSQ1, led to reduced Ca^{2+} storage and release in C2C12 skeletal muscle myotubes. They also found a significant reduction in both the sarco/endoplasmic reticulum Ca^{2+} ATPase (SERCA) and the RyR1 proteins in the CSQ2 knockdown myotubes. Thus, we chose to evaluate CSQ2 instead of CSQ1 for the experiments with C2C12 cells.

Although *in vitro* studies have reported reversible CSQ polymerization and depolymerization, no direct *in vivo* evidence has been obtained to date. Earlier electron microscopy analyses have revealed a fibrous array assumed to be Ca^{2+}-bound CSQ in the SR at the junctional membrane (18). Cross-linking studies have also demonstrated that the majority of CSQ in the SR forms CSQ-CSQ complexes, supporting the physiological relevance of these polymers (14, 19). Here, we transiently overexpressed a fluorescent protein-tagged CSQ2, along with JNT, and examined the *in vivo* dynamics of the macromolecular structure of the CSQ complex using live cell imaging. Our data provide *in vivo* evidence that the occurrence of CSQ2 depolymerization is synchronous with Ca^{2+} depletion and that this conformational change requires coexpression of JNT.

EXPERIMENTAL PROCEDURES

Cell Culture and Transfection—C2C12, a murine skeletal muscle cell line, was grown in Dulbecco's modified Eagle's medium (DMEM; Invitrogen). Media were supplemented with heat-inactivated 10% fetal bovine serum (Invitrogen), non-essential amino acids, 50 units/ml penicillin, and 50 units/ml streptomycin (Invitrogen). Cells were grown at 37 °C and 5% CO_2 and transfected with Lipofectamine reagent (Invitrogen). The amounts of expression plasmids used are specified in the figure legends, and equivalent amounts of plasmid DNA were maintained with a relevant empty vector.

Plasmids and Lentiviral Infection—Human CSQ2 cDNA with a C-terminal yellow fluorescent protein (YFP) fusion was inserted into pLenti M1.4-MCMV, and that containing a C-terminal hemagglutinin (HA) tag was inserted into pcDNA3 vectors for the expression of CSQ2-YFP fusion and CSQ2-HA proteins in mammalian cells, respectively. Mouse JNT cDNA with a C-terminal cyan fluorescent protein (CFP) sequence was inserted into pLenti M1.4-MCMV for the expression of JNT-CFP fusion in mammalian cells. VSV-G-pseudotyped lentivirus was produced in HEK293T cells cotransfected with pLenti M1.4 construct, pLp1, pLp2, and pVSV-G. Culture medium was replaced with serum-free DMEM at 12 h after transfection. Supernatant fractions containing lentivirus particles were collected 48 h later, filtered through a 0.45-μm filter unit, and used to infect C2C12 cells at 60% confluence in the presence of 4 μg/ml of Polybrene or stored at −70 °C.

Immunoprecipitation and Immunoblotting—Cells were harvested, washed with PBS, and lysed in lysis buffer (20 mM HEPES, pH 7.2, 50 mM NaCl, 10% glycerol, 0.5% Triton X-100, 100 μM phenylmethanesulfonyl fluoride, 1 μg/ml each of leupeptin and aprotinin). Lysates were centrifuged and incubated with anti-GFP antibody preincubated with protein A/G-Sepharose (GE Healthcare) or anti-HA-agarose beads (Sigma) for 12 h at 4 °C. Immobilized proteins were collected by centrifugation, washed three times with lysis buffer, and solubilized by boiling for 3 min in SDS-polyacrylamide gel electrophoresis sample buffer. Proteins were separated by electrophoresis on 10–12% SDS-polyacrylamide gels and transferred to nitrocellulose membranes. After blocking with 5% skimmed milk in Tris-buffered saline (20 mM Tris-HCl, pH 7.4, 150 mM NaCl) containing 0.05% Tween 20, membranes were probed with anti-GFP (Santa Cruz Biotechnology), anti-CSQ (Affinity BioReagents), and anti-HA (Sigma) antibodies. Blots were washed with Tris-buffered saline containing Tween 20, incubated with peroxidase-conjugated anti-rabbit IgG (Sigma) antibody, and developed using the chemiluminescence system (Pierce).

Imaging—Imaging was carried out using an inverted confocal microscope (LSM 510 META and LIVE 5, Carl Zeiss) with a 40× objective. To monitor cytosolic Ca^{2+} levels, cells were loaded with 2 μM fluo-4-acetoxymethylester (Fluo-4-AM) (Molecular Probes) in physiological salt solution (150 mM NaCl, 4 mM KCl, 2 mM $CaCl_2$, 1 mM $MgCl_2$, 5 mM glucose, 5 mM HEPES) for 30 min at 37 °C. Fluo-4 was excited with a 488-nm laser line and fluorescence was acquired at wavelengths of 505–530 nm. Cells were treated with thapsigargin (Calbiochem), 2,5-di-(*tert*-butyl)-1,4-benzohydroquinone (Sigma), cyclopiazonic acid (Sigma), or isoproterenol (Sigma) for intracellular Ca^{2+} perturbation. Fluorescence resonance energy transfer (FRET) was measured with the acceptor photobleaching method using CFP and YFP fusion proteins as donor and acceptor, respectively. This method estimates the release of donor quenching after acceptor photobleaching, thus providing a measurement of close colocalization between the fusion proteins. CFP and YFP were excited with the 405- and 514-nm lines of an argon laser, respectively. Emitted fluorescence was collected at 420–480 nm for CFP and 530–600 nm for YFP. Repeated scans with unattenuated 514 nm illumination were used to photobleach YFP. FRET efficiency was estimated using the following equation: $(F_{CFP}\text{Postbleach} - F_{CFP}\text{Prebleach})/F_{CFP}\text{Postbleach} \times 100\%$.

Recombinant CSQ2 and JNT Protein Purification—Human cardiac CSQ2 (NP_001223) (amino acids 20–399) and mouse JNT (AAG40812) without the transmembrane domain (amino acids 68–207) were cloned into pET-28b vector (Novagen) with an N-terminal His_6 tag for affinity purification. For amplification of recombinant CSQ2 and JNT sequences, the following synthetic oligonucleotide primers were used: forward,

5′-GTA GAA CGC AGA ACT CTC ATA TGA AGA GAA CTC AC-3′; and reverse, 5′-CCC CCC CTC GAG GTC GAC CTC GAG **CTA** TTC ATC ATC ATC GTC ATC-3′ for CSQ2; forward, 5′-GTG GCT GTC CAT ATG TTT GAC TTG GTC GAT TAT GAA G-3′, and reverse, 5′-GCC CTT GCT CAC CTC GAG **TCA** GTT CTT TCT CTT C-3′ for JNT. The forward primer introduced a restriction enzyme site for NdeI (underlined), whereas the reverse primer introduced sites for XhoI (underlined) and the stop codon (bold). PCR was performed using *Pfu* DNA polymerase (SolGent) with the following cycling profile: initial denaturation at 95 °C for 2 min, 30 cycles of denaturation at 95 °C for 1 min, annealing at 50 °C for 1 min, elongation at 72 °C for 1 min, and final extension at 72 °C for 10 min. PCR products digested with NdeI and XhoI were inserted into the vector using the corresponding restriction sites. The resulting constructs were verified by DNA sequencing. Prior to the cloning procedure, the first mutation was generated within CSQ2 cDNA to eliminate an undesirable NdeI site by converting CATATG to CTTATG, using the QuikChange II technique (Stratagene). Cells were grown at 37 °C to an optical density (A_{600}) of ~0.6, and protein was induced with 0.2 mM isopropyl β-D-thiogalactopyranoside for 3 h. Next, cells were suspended in 20 mM Tris-Cl (pH 8.0), 500 mM NaCl, and 0.5% Triton X-100 and lysed with sonication. Proteins were subjected to affinity purification with Ni^{2+} affinity chromatography, and the His_6 tag was removed by incubation with thrombin for 12 h at 4 °C. Proteins were subsequently purified using a gel filtration column (HiLoad 16/60, Amersham Biosciences) in final buffer (20 mM HEPES, 150 mM NaCl, 2 mM DTT, pH 7.5) with the FPLC system (Amersham Biosciences).

Atomic Force Microscopy (AFM)—Purified CSQ2 alone and the CSQ2-JNT mixture (10 μM each) were dialyzed against polymerization-inducing buffer (5 mM $CaCl_2$, 150 mM NaCl, 2 mM DTT, 20 mM HEPES, pH 7.5) for 5 h at room temperature. An aliquot of each sample was deposited on film, dried under vacuum, and washed with distilled water. AFM measurements were performed with a Dimension 3100 scanning probe microscope (Digital Instruments Veeco) in tapping mode. Silicon nitride cantilevers were used as square pyramidal tips with a scan rate of 1 Hz for a 500 × 500-nm^2 scale image. The resonance frequency was 320 kHz, and the force constant was 20 newtons/m. Raw AFM data were processed using a flattening/low pass fitting process.

Electron Microscopy (EM)—Purified CSQ2 and CSQ2-JNT mixtures (10 μM each) were incubated in polymerization-inducing buffer with or without 5 mM Ca^{2+}, and the supernatant fractions were isolated by centrifugation. Aliquots (5 μl) of the reactions were applied to glow-discharged carbon-coated grids and negatively stained with 2% (w/v) uranyl acetate solution. Micrographs were recorded with a CCD camera (2k, Gatan) using a Tecnai F20 field emission gun electron microscope operated at 200 kV (FEI).

RESULTS

SR Ca^{2+} Depletion Induces Decondensation of CSQ2 Speckles—To investigate the *in vivo* dynamics of CSQ2 oligomerization in response to perturbation of the Ca^{2+} concentration, CSQ2 was ectopically expressed with a fluorescent protein tag in C2C12 myoblasts, and the real-time fluorescence image was examined with confocal microscopy. As CSQ interacts with JNT or TRN (4, 5) and undergoes assembly into the RyR complex, JNT was cotransfected with CSQ. CSQ appeared as speckles in myoblasts, consistent with a previous finding (20). Ca^{2+} perturbation was performed by treating cells with thapsigargin, which inhibits SERCA, resulting in SR Ca^{2+} depletion within a few minutes and a corresponding transient Ca^{2+} increase in the cytoplasm (21). Upon coexpression with JNT, CSQ speckles became diffuse in live cells after thapsigargin treatment (Fig. 1*A*, *lower panel*; supplemental Movies S1 and S2). Sequential decondensation progression was additionally evident in the high-resolution images of cells fixed at intervals after thapsigargin treatment (Fig. 1*B*). Speckle shapes began to change at 5 min after thapsigargin treatment and became fully diffuse in 30 min (Fig. 1*B*). However, upon expression of CSQ only, speckles remained unchanged following thapsigargin treatment (Fig. 1*A*, *upper panel*). This result suggests that JNT assists in the decondensation of CSQ speckles that occurs upon Ca^{2+} depletion. We examined SR Ca^{2+} release by monitoring fluorescence of Fluo-4 placed in the cytoplasm after thapsigargin treatment. Cells coexpressing CSQ and JNT showed similar patterns of Ca^{2+} transients upon thapsigargin treatment as untransfected control cells (supplemental Fig. S1), implying Ca^{2+} release from SR to the cytoplasm. We speculated that Ca^{2+} release from CSQ induced by thapsigargin promotes changes in the speckle shape. To evaluate the state of CSQ2, we performed native gel electrophoresis of cell lysates expressing CSQ2 (supplemental Fig. S2). As expected, CSQ2 was present in the form of a variety of polymers in a normal condition and was also found in the depolymerized form, which revealed a high content of monomeric CSQ2 following thapsigargin treatment. This finding is consistent with previous *in vitro* experiments showing that lower environmental Ca^{2+} concentrations trigger release of Ca^{2+} from the CSQ polymer, with concomitant disruption of its polymeric structure (3, 14). Other SERCA inhibitors, such as cyclopiazonic acid (22) and 2,5-*t*-butylhydroquinone (23), also affect decondensation of CSQ speckles (Fig. 2, *B* and *C*). However, caffeine, an RyR channel opener, did not alter the CSQ speckle shape. We suggest that the transient Ca^{2+} decrease caused by caffeine treatment is not sufficient (in regard to concentration or duration) to induce major conformational changes in the CSQ polymer but that the irreversible SR Ca^{2+} depletion as a result of treatment with SERCA inhibitors is enough to do so. As JNT is necessary for this process, we examined the stoichiometry of molar interactions for CSQ speckle decondensation. The molar ratio of JNT to CSQ was important in the thapsigargin response. Specifically, when the JNT:CSQ molar ratio approached 1 (Fig. 3), speckle decondensation progressed clearly. However, at significantly lower concentrations of JNT than CSQ (for example, 1:3), speckle decondensation was marginal (Fig. 3). This result is in keeping with previous *in vitro* experiments showing that loss of interactions with JNT (or TRN) induces compact folding of CSQ at high Ca^{2+} concentrations (5). At higher JNT levels than CSQ (for example, 3:1), inefficient speckle decondensation was observed (Fig. 3). Accordingly, we sug-

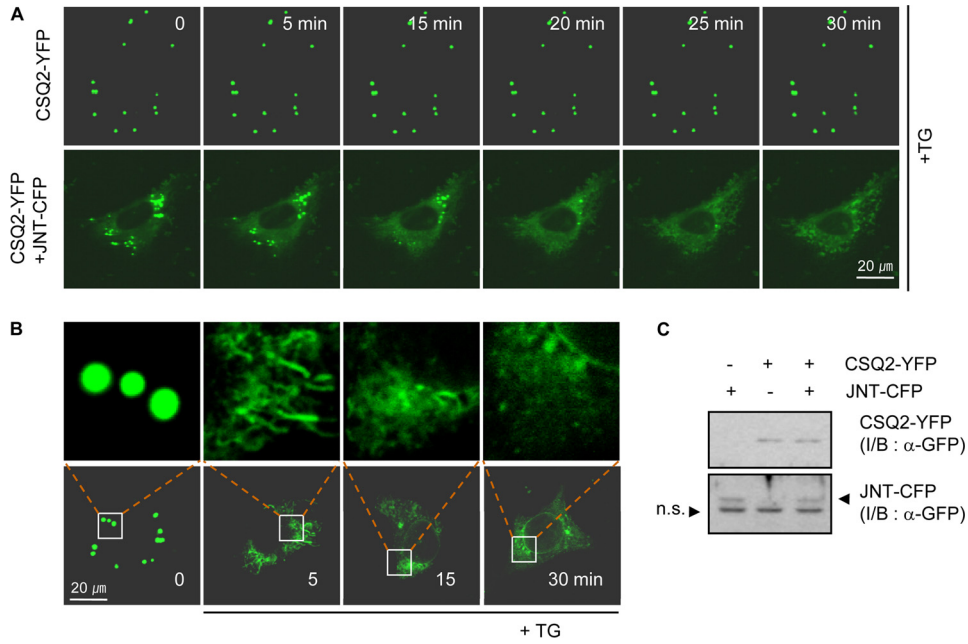

FIGURE 1. **JNT promotes decondensation of CSQ2 speckles upon SR Ca^{2+} depletion.** *A*, time-lapse images of CSQ2 decondensation in the presence of JNT. C2C12 cells expressing YFP-tagged CSQ2 (CSQ2-YFP) with or without CFP-tagged JNT (JNT-CFP) were treated with 5 μM thapsigargin (*TG*), and YFP fluorescence was traced in live cells under live confocal microscopy with incubation for 30 min. *B*, high-resolution images of CSQ2 speckle decondensation in cells coexpressing CSQ and JNT. *Upper panels* represent magnified photographs of the *boxes* in the *lower panels*. Cells cultured on coverslips were treated with thapsigargin, fixed at 5-min intervals, and observed under a confocal microscope. *C*, C2C12 cells were transfected with JNT-CFP and CSQ2-YFP or GFP control vector. At 40 h after transfection, cell lysates were prepared and analyzed by immunoblotting (*I/B*) with anti-GFP antibodies. *n.s.* denotes nonspecific.

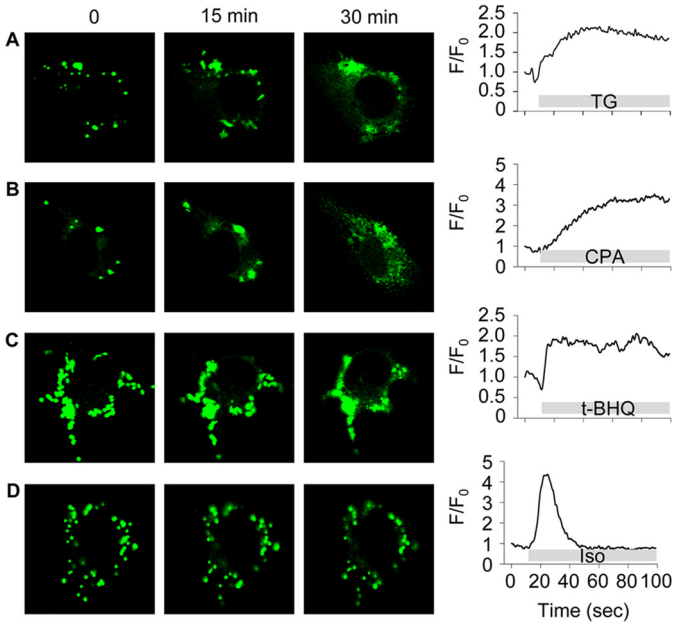

FIGURE 2. **Effects of Ca^{2+} perturbation on decondensation of CSQ2 speckles.** C2C12 myoblasts transfected with CSQ2-YFP and JNT-CFP were treated with SERCA inhibitors, such as thapsigargin (*TG*, 5 μM), cyclopiazonic acid (*CPA*, 10 μM), and 2,5-di-(*tert*-butyl)-1,4-benzohydroquinone (*tBHQ*, 100 μM), or a β-adrenergic receptor agonist isoproterenol (*ISO*, 10 μM). Cells were preincubated with 2 μM Fluo-4 AM for 30 min and washed with 1× physiological salt solution prior to drug treatment for 30 min. CSQ2 decondensation and cytoplasmic Ca^{2+} levels were monitored in cells coexpressing CSQ2-YFP and JNT-CFP using live confocal microscopy.

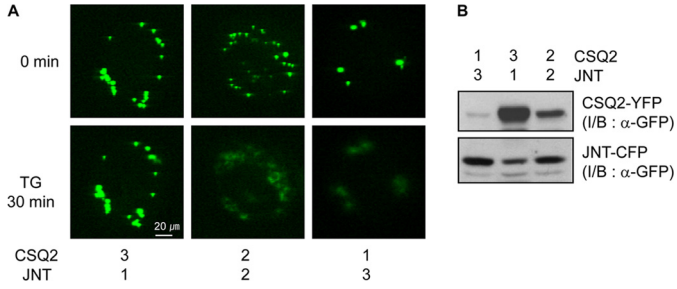

FIGURE 3. **The molar ratios of JNT to CSQ is important for CSQ decondensation.** *A*, decondensation analysis of CSQ2 speckles in C2C12 cells expressing different concentrations of CSQ2-YFP and JNT-CFP. SR Ca^{2+} depletion was induced by thapsigargin (*TG*) treatment. *B*, expression levels of CSQ2-YFP and JNT-CFP were confirmed by immunoblotting (*I/B*) analysis with the anti-GFP antibody. The relative concentrations of proteins are indicated with approximate values.

gest that stoichiometric interactions of CSQ and JNT are necessary for Ca^{2+}-dependent CSQ depolymerization.

CSQ2 Interacts with JNT—To examine the interactions between exogenously expressed CSQ and JNT, C2C12 cells were cotransfected with HA-tagged CSQ2 and CFP-tagged JNT expression plasmids, and coimmunoprecipitation assays were performed. CSQ2 was detected in immunoblots of JNT-CFP immunoprecipitates with the anti-GFP antibody (Fig. 4*A*). In reverse order, JNT was probed in CSQ2-HA immunoprecipitates with the anti-HA antibody (Fig. 4*B*). Thapsigargin treatment did not influence this interaction significantly (Fig. 4*B*, *lane 3 versus lane 4*), suggesting that the levels of CSQ-JNT interactions are maintained, even after disruption of CSQ2 speckles at lower Ca^{2+} concentrations. To determine whether CSQ and JNT proteins colocalize in intact cells, we utilized FRET technology. CSQ2 and JNT were expressed as N-terminal fusions with YFP and CFP, respectively. In an acceptor photobleaching experiment, YFP and CFP fluorescence was monitored before and after YFP was bleached in a region of interest. If CFP and YFP are in close proximity, donor (CFP) fluorescence should increase in the region where the acceptor (YFP) is

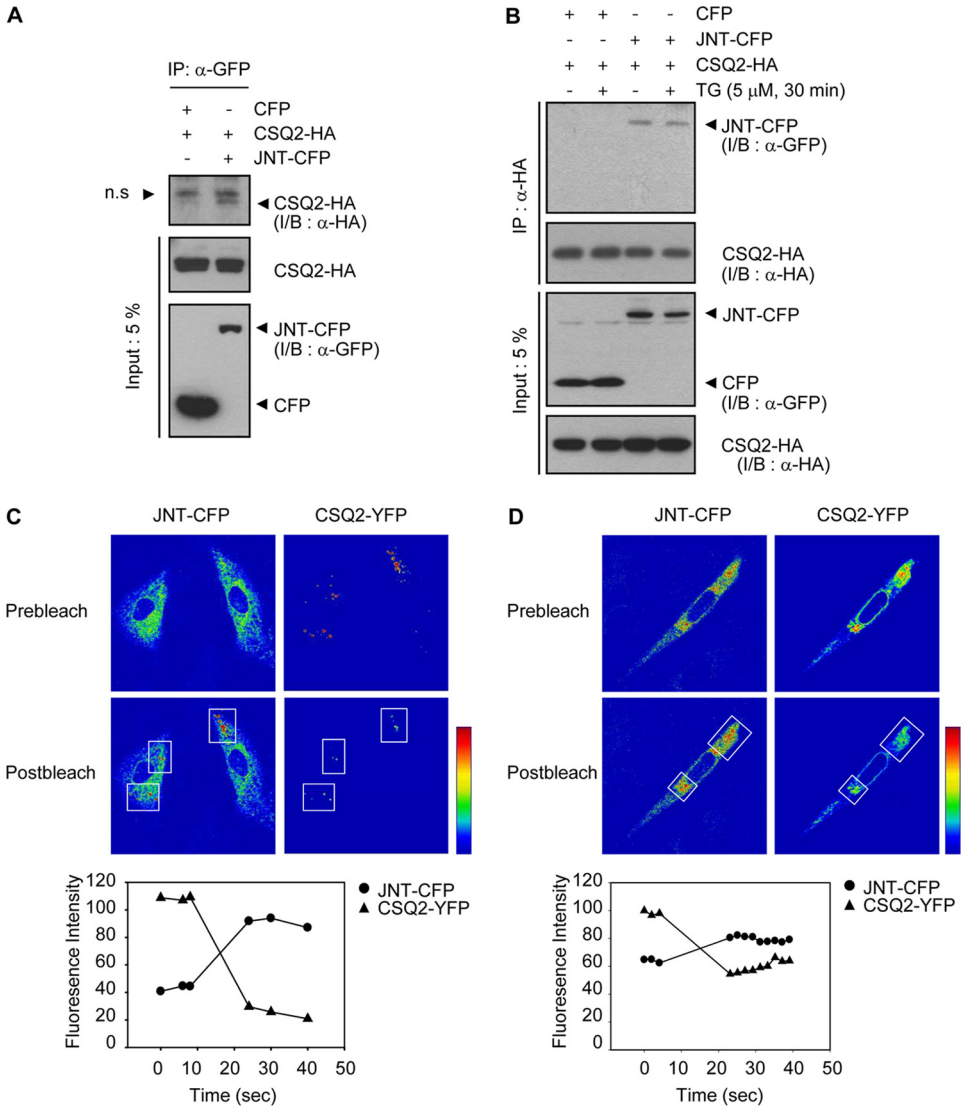

FIGURE 4. **CSQ2 interacts with JNT.** *A*, 293T cells were cotransfected with HA-tagged CSQ2 (CSQ2-HA), together with JNT-CFP or control vector. After 40 h, cells were lysed, and JNT was immunoprecipitated (*IP*) with an anti-GFP antibody. CSQ2 was detected by immunoblotting (*I/B*) with anti-HA antibody. *B*, 293T cells were cotransfected with CSQ2-HA and JNT-CFP or control vector. After 40 h, cells were treated with or without thapsigargin (*TG*) (5 μM) for 30 min prior to lysis, and CSQ2 was immunoprecipitated with an anti-HA antibody. JNT was detected by immunoblotting with an anti-GFP antibody. *C*, FRET analysis to detect interactions between CSQ and JNT. Representative confocal images of CFP and YFP fluorescence were acquired from myoblasts cotransfected with JNT-CFP and CSQ2-YFP fusion constructs before (*upper panels*) and after (*lower panels*) photobleaching of YFP. Images were pseudocolored for easy visualization of fluorescence intensity. The bleached regions of interest are indicated with *white lines*. Fluorescent intensities (●, CFP; ▲, YFP) were measured within a bleached zone at three time points before and after bleaching. Representative plots were drawn with data from the rightmost zone. *D*, FRET analysis was additionally performed under similar conditions after thapsigargin treatment for 30 min. *n.s.* denotes nonspecific.

bleached. JNT-CFP was distributed throughout the cytoplasm, whereas CSQ2-YFP was localized in part of the cytoplasm as speckles (Fig. 4*C*, *upper panels*). After bleaching of the acceptor fluorophore (CSQ2-YFP), which led to almost complete removal of fluorescence intensity (Fig. 4*C*, *lower right panel*), increased fluorescence of donor molecules (JNT-CFP) was detected in the region of acceptor bleaching (Fig. 4*C*, *lower left panel*, *yellow* to *red pseudocolor*). Quantitative analysis revealed that CSQ2-YFP lost its yellow fluorescence by ~80% after bleaching, whereas JNT-CFP gained cyan fluorescence by ~40% (Fig. 4*C*). This result indicates that the two proteins are in close proximity to each other near the speckle positions. To determine whether the interactions between CSQ and JNT proteins remain after decondensation of CSQ speckles, FRET was performed after thapsigargin treatment in cells coexpressing CSQ2-YFP and JNT-CFP. Consistent with immunoprecipitation data, thapsigargin hardly influenced FRET outcome (Fig. 4*D*), suggestive of constant interactions between CSQ and JNT, irrespective of the Ca^{2+} and polymerization states.

Macromolecular Structure of Polymerized CSQ2 in Vitro—Data from the present study showed that CSQ2 speckle decondensation occurs in a Ca^{2+}- and JNT-dependent manner in skeletal muscle cells. We examined this issue *in vitro* using purified proteins. First, we tested the solubility of polymers generated with different concentrations of CSQ2 and JNT. Purified CSQ2 was combined with JNT at different molar ratios or left unmixed. Polymerization proceeded in buffer containing 5 mM Ca^{2+}, as described in the previous study (15). After centrifugation, precipitates and supernatants were separated. Supernatants (Fig. 5*A*, *Soluble I*) were further prepared for negative

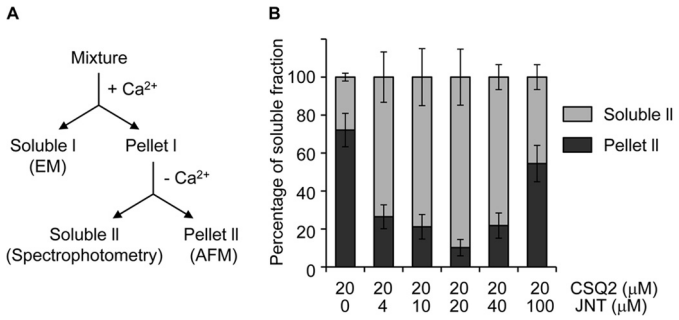

FIGURE 5. **JNT promotes depolymerization of Ca^{2+}-induced CSQ2 polymer.** *A*, scheme of fractionation experiments for analysis of CSQ2 polymerization and depolymerization. CSQ2 (20 μM) and JNT (0–100 μM) were mixed at different molar ratios, incubated in polymerization buffer (5 mM $CaCl_2$, 50 mM KCl, 1 mM DTT, 20 mM Tris-Cl, pH 7.4) at room temperature for 15 min, and spun down at 15,000 $\times$ *g* for 5 min. Precipitated polymers (*Pellet I*) were resolubilized in depolymerization buffer without Ca^{2+} (500 mM KCl, 1 mM EGTA, 20 mM Tris-Cl, pH 7.4), and the soluble II and insoluble pellet II fractions were separated after centrifugation. *B*, stoichiometric analysis of resolubilization of the CSQ2 polymer with JNT. Protein concentrations of the soluble II (*gray*) and pellet II (*dark*) fractions are shown.

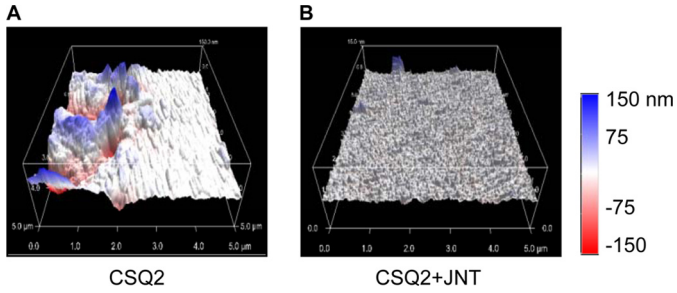

FIGURE 6. **Contribution of JNT to Ca^{2+}-induced CSQ2 polymerization.** Polymers containing CSQ2 alone and both CSQ2 and JNT were examined using AFM. CSQ2 and CSQ2 plus JNT polymers were prepared by dialyzing protein solution (20 μM total protein) against polymerization-inducing buffer and washed with distilled water. Residual precipitates were observed under AFM. Images represent scans of the 5 $\times$ 5-μm area.

staining electron microscopic analysis (see below). To establish whether the precipitation (polymerization) reaction is reversible, precipitates (Fig. 5*A*, *Pellet I*) were incubated in buffer without Ca^{2+}. Resolubilized fractions (*Soluble II*) were separated from insoluble precipitates (*Pellet II*) by centrifugation, and the protein concentrations were measured (Fig. 5*B*). *In vitro* Ca^{2+}-free conditions may mimic the *in vivo* conditions of SR Ca^{2+} depletion (Figs. 1 and 2) that induce solubilization (decondensation) of CSQ speckles. Polymers obtained from equimolar mixtures of CSQ and JNT exhibited highest solubility with the lowest residual precipitates after Ca^{2+} removal (Fig. 5*B*, *fourth bar*, compare *gray* with *dark parts*) among those obtained from mixtures of various molar ratios of CSQ and JNT. The solubilization efficiency gradually decreased as the ratio diverged from equimolar concentrations. A low proportion of polymers generated from CSQ only was converted to the soluble form (<30%), whereas those from the 1:1 CSQ-JNT mixture were susceptible to solubilization (up to 90%). This result is in agreement with our *in vivo* data showing that CSQ-JNT stoichiometry is critical for speckle decondensation. Second, residual precipitates (*Pellet II*) of the CSQ polymers in the presence or absence of JNT were observed under AFM performed to analyze macromolecular structures. In the absence of JNT, significant amounts of large CSQ aggregates (heights of up to 150 nm) were observed in the AFM image (Fig. 6*A*). In contrast, in the presence of JNT, smaller, evenly sized aggregates appeared (Fig. 6*B*). This finding is compatible with data from the solubility test (Fig. 5*B*), indicating that JNT mediates solubilization (destabilization) of the CSQ polymer, both *in vitro* and *in vivo*.

Third, we examined the oligomeric states of the CSQ molecule in the absence or presence of JNT using EM. Protein solutions were incubated with or without 5 mM Ca^{2+}, and their supernatant fractions (*Soluble I*) were isolated by centrifugation to remove insoluble aggregates, mounted, and negatively stained for EM. Previous studies showed that CSQ exists mainly in dimeric, tetrameric, and polymeric states in the presence of 5 mM Ca^{2+} (16). Consistent with earlier findings, we observed dimer-, tetramer-, and oligomer-like structures in EM images (Fig. 7, *B* and *C*). After magnification (Fig. 7, *insets*), CSQ appeared as a propeller-shaped particle (diameter, 60–80 Å) containing three to four globular domains in the presence of 5 mM Ca^{2+}. We assume that the particle corresponds to a front-to-front dimer because dimers having three or four globular domains can be imaged, depending on the direction (angle) of attachment to the grid surface (Fig. 7*B*). The repetitive domain appears to be a thioredoxin-like domain (diameter ~30 Å), previously identified in x-ray crystallography analyses (14). However, no evident structure was observed in the absence of Ca^{2+} (Fig. 7*A*). Previous intrinsic fluorescence, circular dichroism, Raman spectroscopy, NMR, and proteolytic digestion analyses performed to determine the physicochemical properties of CSQ revealed that CSQ is a mostly unfolded random coil at low ionic strength but that it folds into a compact structure with increasing ion concentrations (24–26). This result has been replicated in our EM experiments showing disruption of the thioredoxin-like domain in the absence of Ca^{2+} (Fig. 7*A*). Upon incubation of equal amounts of CSQ and JNT (Fig. 7*C*), the total number of propeller-shaped particles decreased, and the appearance of the high-order structure (chain-like) that prevailed in the CSQ-only sample also decreased (Fig. 7, *B versus C*). Our results consistently suggest that interactions between JNT and CSQ compete with the intermolecular interactions among CSQ, thereby facilitating disassembly or preventing the formation of CSQ polymers.

DISCUSSION

Reversibility is a typical mechanism to maintain homeostasis in biological systems. The bidirectional reactions of CSQ polymerization and depolymerization may thus be critical in Ca^{2+} homeostasis. Previous studies have proposed that positive cooperative binding of Ca^{2+} by CSQ is concomitant with a shift in equilibrium from the soluble to the crystalline forms of CSQ (27), which folds into a more compact structure (28–30). Thus, CSQ polymerization appears beneficial for Ca^{2+} deposit. Based on the crystal structures, various lengths of CSQ polymer are expected to form with increasing Ca^{2+} concentrations (14–16) (PDB 1SJI). These CSQ polymers tend to depolymerize upon lowering of the free Ca^{2+} concentration (15, 31–33). In addition, during FRET analysis of CSQ2 polymerization in cells cotransfected with CFP- and YFP-tagged CSQs, depletion of the endoplasmic reticulum Ca^{2+} stores with ionomycin

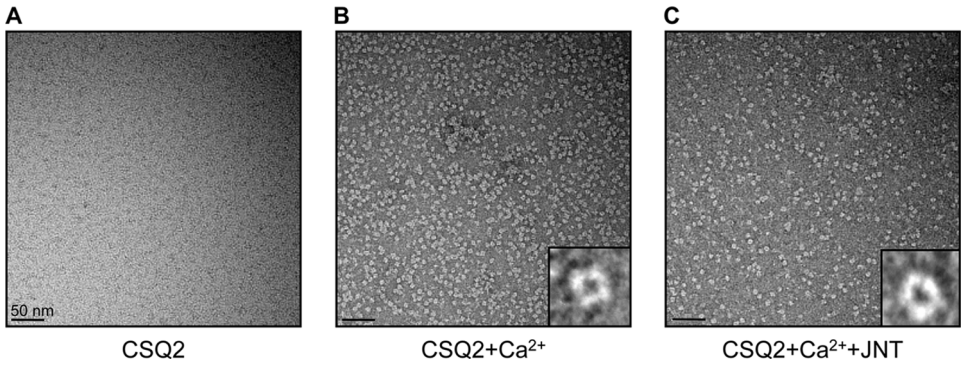

FIGURE 7. **Oligomeric states of the CSQ molecular in the absence or presence of JNT.** *B* and *C*, negatively stained EM images of the soluble fractions of Ca^{2+}-induced CSQ2 polymerization reaction in the absence (*B*) or presence of JNT (*C*). *A*, the Ca^{2+}-free CSQ2 sample was used as a control. *Insets* represent magnified images.

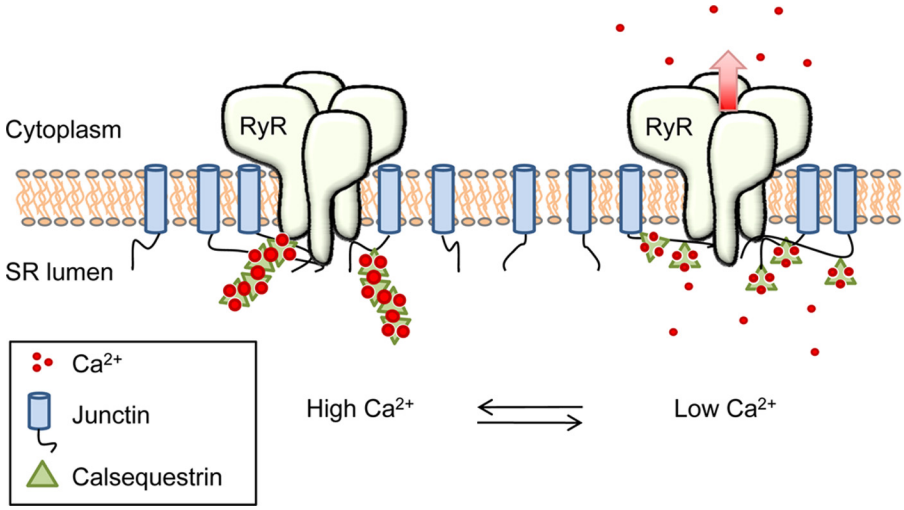

FIGURE 8. **Schematic diagram of CSQ, JNT, and RyR interactions in a junctional face of SR.** At increasing Ca^{2+} concentrations, JNT coordinates with the growing CSQ polymer in the vicinity of a RyR-localizing Ca^{2+} store near the release port. Upon channel opening and deployment of Ca^{2+} ions, CSQ tethered to JNT undergoes depolymerization. CSQ, JNT, and Ca^{2+} are depicted as *triangles*, *blue tubes*, and *red dots*.

resulted in a marked decrease in FRET efficiency, suggestive of CSQ depolymerization (31). Stopped-flow analysis showed that intrinsic CSQ fluorescence decreases with decreasing concentrations of Ca^{2+} from 1 mM to 0.1–100 μM, indicative of depolymerization (32). However, there is no direct evidence of Ca^{2+}-dependent CSQ depolymerization *in vivo* with physiological relevance. Live cell imaging analysis (supplemental Movies S1 and S2 and Fig. 1) suggested JNT-dependent depolymerization of the CSQ polymer *in vivo* after Ca^{2+} depletion. CSQ polymer underwent slow conformational changes upon SR Ca^{2+} depletion using a SERCA inhibitor, and this was not synchronized with the twitches of normal, millisecond-long excitation-contraction coupling. We speculate that complete depolymerization does not occur during excitation-contraction coupling but that partial Ca^{2+} release from CSQ and a corresponding partial depolymerization do occur, which is followed by a rebound in Ca^{2+} and the repolymerization of CSQ. In contrast, under certain pathological conditions, virtually all of the Ca^{2+} becomes lost from CSQ, and this may lead to the full depolymerization of the CSQ polymer without the possibility of reconstruction. In cardiac muscle, it has been shown that the lower intraluminal SR Ca^{2+} concentration characteristic of heart failure results in abnormal CSQ trafficking (34). Irreversible SR Ca^{2+} depletion also occurs in malignant hyperthermia (35), a syndrome evident in mice lacking CSQ (36).

Our data strongly suggest that direct molecular interactions between CSQ and JNT are necessary for CSQ-mediated Ca^{2+} control in SR. JNT-null cardiomyocytes display increased frequency of Ca^{2+} sparks, indicative of increased SR leak, the phenotype of which is associated with arrhythmia (37). JNT-overexpressing cardiomyocytes display depressed contractility and reduced Ca^{2+} in both transient and SR load (38, 39). Consistently, cardiac overexpression of canine JNT in mice results in decreased contractility, impaired relaxation, and hypertrophy (40, 41). Experiments from the current study disclosed that upon overexpression of JNT, interactions between JNT and CSQ increase, inhibiting polymerization of CSQ and leading to reduced SR Ca^{2+} load and reduced spontaneous SR Ca^{2+} release. On the other hand, upon JNT ablation, the bridge between CSQ and RyR may be abolished, resulting in desynchronized SR Ca^{2+} release (42). We showed that the molar ratio of JNT-CSQ is critically important in Ca^{2+}-CSQ dynamics by ectopic coexpression in C2C12 cells (Fig. 3). When the JNT level was significantly higher or lower than the CSQ level, depolymerization barely occurred (Fig. 3), possibly due to abnormal SR Ca^{2+} load and CSQ mislocalization, respectively. Pre-

viously, CSQ condensation was observed in L6 myoblast and HeLa cells transfected with CSQ, which remained unchanged after depletion of endoplasmic reticulum Ca^{2+} stores (20), possibly due to imbalance in the levels of CSQ relative to JNT. We replicated the necessity for JNT in CSQ depolymerization reactions *in vitro* in experiments using the purified proteins (Figs. 5–7). Reversible CSQ polymerization and depolymerization were dependent on the Ca^{2+} concentration and JNT-CSQ ratios, consistent with *in vivo* data (Figs. 1–3).

The stoichiometry of the RyR complex has been studied in detail. FKBP12 (or FKBP12.6), calmodulin, TRN, and JNT are each known to interact with the RyR subunit in a 1:1 manner (5, 43–45). Both transgenic and knock-out mouse models of CSQ2 have demonstrated significantly decreased TRN and JNT protein levels (46, 47). TRN knock-out mice also have significantly decreased CSQ2 and JNT protein levels (48). These results suggest a potential interdependence between these three proteins. Furthermore, CSQ function is known to depend on the stoichiometry of the association with the RyR-TRN-JNT-CSQ macromolecular complex (49). Here, we found that the stoichiometric interaction of CSQ2 with JNT was critical for the CSQ2 depolymerization reaction *in vivo* and have suggested that the optimal ratio of JNT-CSQ expression for this reaction is 1:1 (protein levels). However, endogenous JNT is present at lower levels than endogenous CSQ under physiological conditions (49–51). A possible explanation, which may reconcile the difference between physiological conditions and our experimental conditions, is seen in Fig. 8. It is likely that some JNT molecules remain free, whereas others interact with polymerized CSQ. Thus, the final interaction of JNT and CSQ may be at a ratio less than 1:1. This suggestion is in line with our *in vivo* imaging data showing that ectopically expressed JNT is diffusely expressed, whereas that of CSQ is speckled (Fig. 4, *C* and *D*). Thus, the limited concentrations of endogenous JNT *in vivo* might be necessary and sufficient to play key roles in the reversible dynamics of Ca^{2+}-CSQ polymerization and depolymerization, which are located adjacent to RyR.

Acknowledgments—We thank Jae-Seok Ha for confocal microscopy and Gil Bu Kang for calsequestrin protein preparations.

REFERENCES

1. Beard, N. A., Wei, L., and Dulhunty, A. F. (2009) Ca^{2+} signaling in striated muscle: the elusive roles of triadin, junctin, and calsequestrin. *Eur. Biophys. J.* **39,** 27–36
2. MacLennan, D. H., and Wong, P. T. (1971) Isolation of a calcium-sequestering protein from sarcoplasmic reticulum. *Proc. Natl. Acad. Sci. U.S.A.* **68,** 1231–1235
3. Beard, N. A., Laver, D. R., and Dulhunty, A. F. (2004) Calsequestrin and the calcium release channel of skeletal and cardiac muscle. *Prog Biophys Mol. Biol.* **85,** 33–69
4. Guo, W., and Campbell, K. P. (1995) Association of triadin with the ryanodine receptor and calsequestrin in the lumen of the sarcoplasmic reticulum. *J. Biol. Chem.* **270,** 9027–9030
5. Zhang, L., Kelley, J., Schmeisser, G., Kobayashi, Y. M., and Jones, L. R. (1997) Complex formation between junctin, triadin, calsequestrin, and the ryanodine receptor. Proteins of the cardiac junctional sarcoplasmic reticulum membrane. *J. Biol. Chem.* **272,** 23389–23397
6. Glover, L., Culligan, K., Cala, S., Mulvey, C., and Ohlendieck, K. (2001) Calsequestrin binds to monomeric and complexed forms of key calcium-handling proteins in native sarcoplasmic reticulum membranes from rabbit skeletal muscle. *Biochim. Biophys. Acta* **1515,** 120–132
7. Györke, I., Hester, N., Jones, L. R., and Györke, S. (2004) The role of calsequestrin, triadin, and junctin in conferring cardiac ryanodine receptor responsiveness to luminal calcium. *Biophys. J.* **86,** 2121–2128
8. di Barletta, M. R., Viatchenko-Karpinski, S., Nori, A., Memmi, M., Terentyev, D., Turcato, F., Valle, G., Rizzi, N., Napolitano, C., Gyorke, S., Volpe, P., and Priori, S. G. (2006) Clinical phenotype and functional characterization of CASQ2 mutations associated with catecholaminergic polymorphic ventricular tachycardia. *Circulation* **114,** 1012–1019
9. Lahat, H., Pras, E., Olender, T., Avidan, N., Ben-Asher, E., Man, O., Levy-Nissenbaum, E., Khoury, A., Lorber, A., Goldman, B., Lancet, D., and Eldar, M. (2001) A missense mutation in a highly conserved region of *CASQ2* is associated with autosomal recessive catecholamine-induced polymorphic ventricular tachycardia in Bedouin families from Israel. *Am. J. Hum. Genet.* **69,** 1378–1384
10. Postma, A. V., Denjoy, I., Hoorntje, T. M., Lupoglazoff, J. M., Da Costa, A., Sebillon, P., Mannens, M. M., Wilde, A. A., and Guicheney, P. (2002) Absence of calsequestrin 2 causes severe forms of catecholaminergic polymorphic ventricular tachycardia. *Circ. Res.* **91,** e21–26
11. Terentyev, D., Nori, A., Santoro, M., Viatchenko-Karpinski, S., Kubalova, Z., Gyorke, I., Terentyeva, R., Vedamoorthyrao, S., Blom, N. A., Valle, G., Napolitano, C., Williams, S. C., Volpe, P., Priori, S. G., and Gyorke, S. (2006) Abnormal interactions of calsequestrin with the ryanodine receptor calcium release channel complex linked to exercise-induced sudden cardiac death. *Circ. Res.* **98,** 1151–1158
12. Kirchhof, P., Klimas, J., Fabritz, L., Zwiener, M., Jones, L. R., Schäfers, M., Hermann, S., Boknik, P., Schmitz, W., Breithardt, G., Kirchhefer, U., and Neumann, J. (2007) Stress and high heart rate provoke ventricular tachycardia in mice expressing triadin. *J. Mol. Cell Cardiol* **42,** 962–971
13. Scott, B. T., Simmerman, H. K., Collins, J. H., Nadal-Ginard, B., and Jones, L. R. (1988) Complete amino acid sequence of canine cardiac calsequestrin deduced by cDNA cloning. *J. Biol. Chem.* **263,** 8958–8964
14. Wang, S., Trumble, W. R., Liao, H., Wesson, C. R., Dunker, A. K., and Kang, C. H. (1998) Crystal structure of calsequestrin from rabbit skeletal muscle sarcoplasmic reticulum. *Nat. Struct. Biol.* **5,** 476–483
15. Park, H., Wu, S., Dunker, A. K., and Kang, C. (2003) Polymerization of calsequestrin. Implications for Ca^{2+} regulation. *J. Biol. Chem.* **278,** 16176–16182
16. Park, H., Park, I. Y., Kim, E., Youn, B., Fields, K., Dunker, A. K., and Kang, C. (2004) Comparing skeletal and cardiac calsequestrin structures and their calcium binding: a proposed mechanism for coupled calcium binding and protein polymerization. *J. Biol. Chem.* **279,** 18026–18033
17. Wang, Y., Xu, L., Duan, H., Pasek, D. A., Eu, J. P., and Meissner, G. (2006) Knocking down type 2 but not type 1 calsequestrin reduces calcium sequestration and release in C2C12 skeletal muscle myotubes. *J. Biol. Chem.* **281,** 15572–15581
18. Franzini-Armstrong, C., Kenney, L. J., and Varriano-Marston, E. (1987) The structure of calsequestrin in triads of vertebrate skeletal muscle: a deep-etch study. *J. Cell Biol.* **105,** 49–56
19. Maguire, P. B., Briggs, F. N., Lennon, N. J., and Ohlendieck, K. (1997) Oligomerization is an intrinsic property of calsequestrin in normal and transformed skeletal muscle. *Biochem. Biophys. Res. Commun.* **240,** 721–727
20. Gatti, G., Podini, P., and Meldolesi, J. (1997) Overexpression of calsequestrin in L6 myoblasts: formation of endoplasmic reticulum subdomains and their evolution into discrete vacuoles where aggregates of the protein are specifically accumulated. *Mol. Biol. Cell* **8,** 1789–1803
21. Thastrup, O., Cullen, P. J., Drøbak, B. K., Hanley, M. R., and Dawson, A. P. (1990) Thapsigargin, a tumor promoter, discharges intracellular Ca^{2+} stores by specific inhibition of the endoplasmic reticulum Ca^{2+}-ATPase. *Proc. Natl. Acad. Sci. U.S.A.* **87,** 2466–2470
22. Seidler, N. W., Jona, I., Vegh, M., and Martonosi, A. (1989) Cyclopiazonic acid is a specific inhibitor of the Ca^{2+}-ATPase of sarcoplasmic reticulum. *J. Biol. Chem.* **264,** 17816–17823
23. Moore, G. A., McConkey, D. J., Kass, G. E., O'Brien, P. J., and Orrenius, S. (1987) 2,5-Di(*tert*-butyl)-1,4-benzohydroquinone: a novel inhibitor of liver microsomal Ca^{2+} sequestration. *FEBS Lett.* **224,** 331–336

24. Aaron, B. M., Oikawa, K., Reithmeier, R. A., and Sykes, B. D. (1984) Characterization of skeletal muscle calsequestrin by ^{1}H NMR spectroscopy. *J. Biol. Chem.* **259,** 11876–11881
25. He, Z., Dunker, A. K., Wesson, C. R., and Trumble, W. R. (1993) Ca^{2+}-induced folding and aggregation of skeletal muscle sarcoplasmic reticulum calsequestrin. The involvement of the trifluoperazine-binding site. *J. Biol. Chem.* **268,** 24635–24641
26. Ikemoto, N., Nagy, B., Bhatnagar, G. M., and Gergely, J. (1974) Studies on a metal-binding protein of the sarcoplasmic reticulum. *J. Biol. Chem.* **249,** 2357–2365
27. Tanaka, M., Ozawa, T., Maurer, A., Cortese, J. D., and Fleischer, S. (1986) Apparent cooperativity of Ca^{2+} binding associated with crystallization of Ca^{2+}-binding protein from sarcoplasmic reticulum. *Arch. Biochem. Biophys.* **251,** 369–378
28. Mitchell, R. D., Simmerman, H. K., and Jones, L. R. (1988) Ca^{2+} binding effects on protein conformation and protein interactions of canine cardiac calsequestrin. *J. Biol. Chem.* **263,** 1376–1381
29. Cozens, B., and Reithmeier, R. A. (1984) Size and shape of rabbit skeletal muscle calsequestrin. *J. Biol. Chem.* **259,** 6248–6252
30. Ohnishi, M., and Reithmeier, R. A. (1987) Fragmentation of rabbit skeletal muscle calsequestrin: spectral and ion binding properties of the carboxyl-terminal region. *Biochemistry* **26,** 7458–7465
31. Launikonis, B. S., Zhou, J., Royer, L., Shannon, T. R., Brum, G., and Ríos, E. (2006) Depletion "skraps" and dynamic buffering inside the cellular calcium store. *Proc. Natl. Acad. Sci. U.S.A.* **103,** 2982–2987
32. Terentyev, D., Kubalova, Z., Valle, G., Nori, A., Vedamoorthyrao, S., Terentyeva, R., Viatchenko-Karpinski, S., Bers, D. M., Williams, S. C., Volpe, P., and Gyorke, S. (2008) Modulation of SR calcium release by luminal calcium and calsequestrin in cardiac myocytes: effects of CASQ2 mutations linked to sudden cardiac death. *Biophys. J.* **95,** 2037–2048
33. Wei, L., Varsányi, M., Dulhunty, A. F., and Beard, N. A. (2006) The conformation of calsequestrin determines its ability to regulate skeletal ryanodine receptors. *Biophys. J.* **91,** 1288–1301
34. Kiarash, A., Kelly, C. E., Phinney, B. S., Valdivia, H. H., Abrams, J., and Cala, S. E. (2004) Defective glycosylation of calsequestrin in heart failure. *Cardiovasc Res.* **63,** 264–272
35. Duke, A. M., Hopkins, P. M., Calaghan, S. C., Halsall, J. P., and Steele, D. S. (2010) Store-operated Ca^{2+} entry in malignant hyperthermia-susceptible human skeletal muscle. *J. Biol. Chem.* **285,** 25645–25653
36. Canato, M., Scorzeto, M., Giacomello, M., Protasi, F., Reggiani, C., and Stienen, G. J. (2010) Massive alterations of sarcoplasmic reticulum free calcium in skeletal muscle fibers lacking calsequestrin revealed by a genetically encoded probe. *Proceedings of the National Academy of Sciences of the United States of America* **107,** 22326–22331
37. Yuan, Q., Fan, G. C., Dong, M., Altschafl, B., Diwan, A., Ren, X., Hahn, H. H., Zhao, W., Waggoner, J. R., Jones, L. R., Jones, W. K., Bers, D. M., Dorn, G. W. 2nd, Wang, H. S., Valdivia, H. H., Chu, G., and Kranias, E. G. (2007) Sarcoplasmic reticulum calcium overloading in junctin deficiency enhances cardiac contractility but increases ventricular automaticity. *Circulation* **115,** 300–309
38. Fan, G. C., Yuan, Q., Zhao, W., Chu, G., and Kranias, E. G. (2007) Junctin is a prominent regulator of contractility in cardiomyocytes. *Biochem. Biophys. Res. Commun.* **352,** 617–622
39. Gergs, U., Berndt, T., Buskase, J., Jones, L. R., Kirchhefer, U., Müller, F. U., Schlüter, K. D., Schmitz, W., and Neumann, J. (2007) On the role of junctin in cardiac Ca^{2+} handling, contractility, and heart failure. *Am. J. Physiol. Heart Circ Physiol* **293,** H728–H734
40. Hong, C. S., Cho, M. C., Kwak, Y. G., Song, C. H., Lee, Y. H., Lim, J. S., Kwon, Y. K., Chae, S. W., and Kim, D. H. (2002) Cardiac remodeling and atrial fibrillation in transgenic mice overexpressing junctin. *FASEB J.* **16,** 1310–1312
41. Kirchhefer, U., Neumann, J., Bers, D. M., Buchwalow, I. B., Fabritz, L., Hanske, G., Justus, I., Riemann, B., Schmitz, W., and Jones, L. R. (2003) Impaired relaxation in transgenic mice overexpressing junctin. *Cardiovasc Res* **59,** 369–379
42. Pritchard, T. J., and Kranias, E. G. (2009) Junctin and the histidine-rich Ca^{2+}-binding protein: potential roles in heart failure and arrhythmogenesis. *J Physiol* **587,** 3125–3133
43. Chen, S. R., and MacLennan, D. H. (1994) Identification of calmodulin-, Ca^{2+}-, and ruthenium red-binding domains in the Ca^{2+} release channel (ryanodine receptor) of rabbit skeletal muscle sarcoplasmic reticulum. *J. Biol. Chem.* **269,** 22698–22704
44. Lee, E. H., Rho, S. H., Kwon, S. J., Eom, S. H., Allen, P. D., and Kim do, H. (2004) N-terminal region of $FKBP_{12}$ is essential for binding to the skeletal ryanodine receptor. *J. Biol. Chem.* **279,** 26481–26488
45. Timerman, A. P., Onoue, H., Xin, H. B., Barg, S., Copello, J., Wiederrecht, G., and Fleischer, S. (1996) Selective binding of $FKBP_{12.6}$ by the cardiac ryanodine receptor. *J. Biol. Chem.* **271,** 20385–20391
46. Jones, L. R., Suzuki, Y. J., Wang, W., Kobayashi, Y. M., Ramesh, V., Franzini-Armstrong, C., Cleemann, L., and Morad, M. (1998) Regulation of Ca^{2+} signaling in transgenic mouse cardiac myocytes overexpressing calsequestrin. *J. Clin. Invest.* **101,** 1385–1393
47. Knollmann, B. C., Chopra, N., Hlaing, T., Akin, B., Yang, T., Ettensohn, K., Knollmann, B. E., Horton, K. D., Weissman, N. J., Holinstat, I., Zhang, W., Roden, D. M., Jones, L. R., Franzini-Armstrong, C., and Pfeifer, K. (2006) *Casq2* deletion causes sarcoplasmic reticulum volume increase, premature Ca^{2+} release, and catecholaminergic polymorphic ventricular tachycardia. *J. Clin. Invest.* **116,** 2510–2520
48. Knollmann, B. C. (2009) New roles of calsequestrin and triadin in cardiac muscle. *J Physiol* **587,** 3081–3087
49. Knudson, C. M., Stang, K. K., Moomaw, C. R., Slaughter, C. A., and Campbell, K. P. (1993) Primary structure and topological analysis of a skeletal muscle-specific junctional sarcoplasmic reticulum glycoprotein (triadin). *J. Biol. Chem.* **268,** 12646–12654
50. Jones, L. R., Zhang, L., Sanborn, K., Jorgensen, A. O., and Kelley, J. (1995) Purification, primary structure, and immunological characterization of the 26-kDa calsequestrin binding protein (junctin) from cardiac junctional sarcoplasmic reticulum. *J. Biol. Chem.* **270,** 30787–30796
51. Zhang, L., Franzini-Armstrong, C., Ramesh, V., and Jones, L. R. (2001) Structural alterations in cardiac calcium release units resulting from overexpression of junctin. *J Mol Cell Cardiol* **33,** 233–247